Layanan Perpustakaan UHAMKA

CFD simulation for optimizing the evaporation process in seawater desalination using exhaust heat from AC and vortex ...

📋 LK BU OKTA

🖥 Fakultas Teknologi Industri dan Informatika

🎓 Universitas Muhammadiyah Prof. Dr. Hamka

Document Details

Submission ID

trn:oid:::1:3241937419

Submission Date

May 7, 2025, 8:29 AM GMT+7

Download Date

May 7, 2025, 8:36 AM GMT+7

File Name

CFD_simulation_for_optimizing_the_evaporation_process_in_seawater.pdf

File Size

8.0 MB

9 Pages

6,155 Words

34,969 Characters

11% Overall Similarity

The combined total of all matches, including overlapping sources, for each database.

Filtered from the Report

▸ Bibliography

Exclusions

▸ 3 Excluded Sources

▸ 8 Excluded Matches

Match Groups

38 Not Cited or Quoted 8%
Matches with neither in-text citation nor quotation marks

13 Missing Quotations 3%
Matches that are still very similar to source material

0 Missing Citation 0%
Matches that have quotation marks, but no in-text citation

0 Cited and Quoted 0%
Matches with in-text citation present, but no quotation marks

Top Sources

8% 🌐 Internet sources

7% 📖 Publications

2% 👤 Submitted works (Student Papers)

Integrity Flags

1 Integrity Flag for Review

🚩 **Replaced Characters**
20 suspect characters on 1 page
Letters are swapped with similar characters from another alphabet.

Our system's algorithms look deeply at a document for any inconsistencies that would set it apart from a normal submission. If we notice something strange, we flag it for you to review.

A Flag is not necessarily an indicator of a problem. However, we'd recommend you focus your attention there for further review.

Match Groups

🔴 **38** Not Cited or Quoted 8%
Matches with neither in-text citation nor quotation marks

🟠 **13** Missing Quotations 3%
Matches that are still very similar to source material

🟡 **0** Missing Citation 0%
Matches that have quotation marks, but no in-text citation

🟢 **0** Cited and Quoted 0%
Matches with in-text citation present, but no quotation marks

Top Sources

8%	🌐 Internet sources
7%	📖 Publications
2%	👤 Submitted works (Student Papers)

Top Sources

The sources with the highest number of matches within the submission. Overlapping sources will not be displayed.

1 Internet
repository.uhamka.ac.id **3%**

2 Publication
Silvana Dwi Nurherdiana, Alya Rahimah, Ramadhanu Dirja, Kun Prasasti Tungga ... **1%**

3 Publication
Junrong Yang, Tianming Zhong, Xin Yan, Haokun Li, Zhilin He, Haoxian Bai, Shiwe... **<1%**

4 Publication
Weisong Ling, Wei Zhou, Chengzhong Liu, Fang Zhou, Ding Yuan, Jiale Huang. "Str... **<1%**

5 Internet
semarakilmu.com.my **<1%**

6 Publication
Kartik Srivastava, Rashmi Rekha Sahoo. "Experimental and numerical study on th... **<1%**

7 Internet
ltu.diva-portal.org **<1%**

8 Internet
okina.univ-angers.fr **<1%**

9 Publication
Chengji Zong, He Li, Weitang Song, Shumei Zhao, Jiarui Lu, Qiangwei Ma. "Study o... **<1%**

10 Publication
Rohit Kumar, Manmohan Pandey. "Numerical analysis of heat transfer and fluid f... **<1%**

11	Student papers	
Academic Library Consortium		<1%

12	Internet	
www.gdcr.ac.in		<1%

13	Publication	
Xiaofei Liu, Zhongchao Zhao, Cong Li, Jiahui Ding, Xiaojun Pu. "Investigation of lo...		<1%

14	Internet	
ijettjournal.org		<1%

15	Internet	
pubs.aip.org		<1%

16	Publication	
Yucheng Wang, Wensheng Zhao, Pengfei Wang, Jin Jiang, Xiangyu Luo. "Thermal ...		<1%

17	Publication	
Peng Ran, Yingbing Lai, Minchuan Li, Wei Liu, Zhuizhui Jiao, Ying Zhong, Daming ...		<1%

18	Publication	
Purnaning Tuwuh Triwigati, Soyoung Noh, Gyudae Sim, Jiwoo Lee, Eunae Kim, Se...		<1%

19	Internet	
mdpi-res.com		<1%

20	Internet	
www.mdpi.com		<1%

21	Publication	
H. Karkaba, T. Dbouk, C. Habchi, S. Russeil, T. Lemenand, D. Bougeard. "Multi obje...		<1%

22	Publication	
Kwame Nana Opoku, Yidan Wei, Clara Afia Amoah Dankwa, Ruiting Ni et al. "Adv...		<1%

23	Publication	
S. Ya Misyura, V.S. Morozov, P.S. Nagibin, E.R. Podgornaya, N.E. Shlegel, P.A. Strizh...		<1%

24	Internet	
c.coek.info		<1%

25	Internet	
dokumen.pub		<1%

26	Internet	
server.thermalfluidscentral.com		<1%

27	Internet	
wiredspace.wits.ac.za		<1%

28	Publication	
Jiangbo Wang, Ting Fu, Liangcai Zeng, Yuting He. "Power consumption and therm...		<1%

29	Publication	
S. Hamidouche, J. V. Simo Tala, S. Russeil. "Analysis of flow characteristics downst...		<1%

30	Publication	
"Computational Fluid Dynamics", Springer Science and Business Media LLC, 1992		<1%

31	Student papers	
University of Al-Qadisiyah		<1%
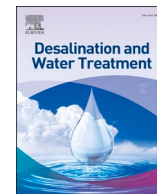
CFD simulation for optimizing the evaporation process in seawater desalination using exhaust heat from AC and vortex generators

Oktarina Heriyani, Dan Mugisidi [*], Rifky

Department of Mechanical Engineering, Faculty of Industrial and Informatics Technology, Universitas Muhammadiyah Prof. DR. HAMKA, Jakarta, Indonesia

HIGHLIGHTS

- Rapid global population growth significantly increases the demand for clean water.
- This study introduces a method to repurpose waste heat from air conditioners for seawater desalination.
- Vortex generators improve evaporation rates by increasing airflow velocity and turbulence.
- CFD simulations confirm the effectiveness of this approach for household-scale desalination systems.

ARTICLE INFO

ABSTRACT

Water is essential for human survival, yet freshwater resources are scarce and limited. In Indonesia's coastal regions, only 66.54 % of the population has access to clean water, highlighting a significant challenge. This issue is further intensified by global warming, which has increased dependence on air conditioners, resulting in substantial waste heat emissions. While often overlooked, this waste heat contributes to local warming and presents an untapped energy resource. Repurposing this energy for innovative applications, such as seawater desalination, offers a promising solution to mitigate clean water shortages. This study proposes using waste heat from household ACs for seawater desalination through evaporation, enhanced by vortex generators. The research examines variations with and without vortex generators across different cross-sectional areas, affecting airflow velocity. Results indicate that using vortex generators significantly increases evaporation rates at all wind speeds. These devices enhance airflow velocity and turbulence, boosting heat transfer and accelerating evaporation. Through Computational Fluid Dynamics (CFD) simulations, the research aims to demonstrate how vortex generators can improve evaporation, offering a practical solution for cooling and desalination at a household scale. This novel approach could significantly benefit water-scarce regions, providing an efficient, cost-effective solution utilising existing household technology.

1. Introduction

Water is a vital substance needed by humans and other living organisms. With the growth of the global population, the water demand has increased rapidly. Estimates show that a 15 % increase in the world population will reduce the availability of clean water by 40 % [1], while the amount of freshwater constitutes only 2.8 % [2] of the total water on the Earth's surface. Because water is so essential, water scarcity can trigger humanitarian, political, and even racial issues [3]. Water scarcity poses a significant global threat and increasingly impacts regions in Indonesia.

As an archipelagic country with the longest coastline in the world,

Indonesia is home to many communities residing in coastal areas. However, they face serious problems related to water scarcity. Only about 66.54 % of them have access to clean water, forcing the majority of coastal residents to use murky and saline water for daily needs such as washing and bathing, while for drinking water, they have to purchase it [4]. Water scarcity is just one of the various problems faced by coastal populations in Indonesia. Global warming is another current issue.

Global warming has transitioned from a potential threat to an urgent global crisis. The Earth's temperature has increased significantly in the past three decades [5]. This temperature rise has caused climate change and is linked to the increasing incidence of severe weather events [6]. In addition, the higher temperatures increase the demand for air

* Corresponding author.
E-mail address: dan.mugisidi@uhamka.ac.id (D. Mugisidi).

conditioning (AC), especially in tropical regions like Indonesia. However, it should be noted that the AC units currently used in households and industries also emit hot air. This is due to the working principle of AC or heat pumps that take hot air from inside the room and expel it outside [7]. Therefore, this research will use heat pumps' waste hot air to evaporate seawater. The resulting vapour will then be condensed to produce clean water. Previous studies have shown that airflow is very adequate in the evaporation process [8]. The problem to be investigated is how to use the waste hot air from ACS to produce clean water through the desalination process, particularly for coastal communities in Indonesia.

Several studies have been conducted using heat pumps for desalination and cooling rooms. Heat pumps have been combined with multistage flash (MSF) and membrane distillation (MD) [9] for cooling and desalination processes. Srinivas used a staged system for desalination and cooling [10]. Junling combined heat pumps with vacuum to process wastewater [11], while several researchers only used heat pumps as desalination units [12,13,14]. However, heat pumps are used only at a large scale for air cooling and desalination. In contrast, Indonesia and many other places use heat pumps or ACs more commonly used for residential purposes.

Therefore, this research proposes a problem-solving approach to using household-scale AC units as air conditioners and desalination units by utilising the hot air released by the AC. The evaporation process will be integrated with a vortex generator to accelerate it. Thus, the second problem to be investigated in this research is integrating vortex generator technology to enhance the evaporation process in desalination units so that clean water can be produced efficiently without compromising AC performance.

The vortex generator is a component that disrupts the flow and increases flow velocity [15], leading to vorticity [16] that reduces flow pressure [17]. Vortex generators have been shown to enhance heat transfer, such as in cooling tower ducts and air channels [18]. Furthermore, since the evaporation pressure at the water surface is greater than the pressure in its surroundings [19] the reduction in flow pressure with the presence of a vortex generator will accelerate the evaporation process.

Based on the literature review, no household-scale desalination unit has used evaporation solely through flow integrated with a vortex generator, whether using a heat pump or not. This represents a novelty in developing more efficient and affordable desalination technology in this research. Additionally, computational fluid dynamics (CFD) simulations will be employed to obtain research results, allowing for a detailed analysis of the airflow dynamics and the impact of the vortex generator on the evaporation rate.

2. Methodology

This study utilises Ansys CFD software to conduct simulations. The basic governing equations of flow through the channel are summarised in terms of continuity, momentum and energy balance equation as follows:

The continuity equation,

$$\frac{\partial}{\partial t}\iiint_V \rho \, dV + \iint_A \rho \vec{V} \bullet d\vec{A} = 0 \tag{1}$$

$$\frac{\partial \rho}{\partial t} + \rho \vec{\nabla} \bullet \vec{V} = 0 \tag{2}$$

The momentum equation in the x-axis direction

$$\frac{\partial(\rho u)}{\partial t} + \vec{\nabla} \bullet \left(\rho u \vec{V}\right) = -\frac{\partial p}{\partial x} + \frac{\partial \tau_{xx}}{\partial x} + \frac{\partial \tau_{yx}}{\partial y} + \frac{\partial \tau_{zx}}{\partial z} + \rho f_x \tag{3}$$

The momentum equation in the y-axis direction

$$\frac{\partial(\rho v)}{\partial t} + \vec{\nabla} \bullet \left(\rho v \vec{V}\right) = -\frac{\partial p}{\partial y} + \frac{\partial \tau_{xy}}{\partial x} + \frac{\partial \tau_{yy}}{\partial y} + \frac{\partial \tau_{zy}}{\partial z} + \rho f_y \tag{4}$$

The momentum equation in the z-axis direction

$$\frac{\partial(\rho w)}{\partial t} + \vec{\nabla} \bullet \left(\rho w \vec{V}\right) = -\frac{\partial p}{\partial z} + \frac{\partial \tau_{xz}}{\partial x} + \frac{\partial \tau_{yz}}{\partial y} + \frac{\partial \tau_{zz}}{\partial z} + \rho f_z \tag{5}$$

The energy equation written in terms of internal energy.

$$\frac{\partial}{\partial t}\left[\rho\left(e + \frac{V^2}{2}\right)\right] + \vec{\nabla} \bullet \left[\rho\left(e + \frac{V^2}{2}\right)\vec{V}\right]$$
$$= \rho\dot{q} - \frac{\partial(\rho p)}{\partial x} - \frac{\partial(vp)}{\partial y} - \frac{\partial(wp)}{\partial z} + \rho\vec{f} \bullet \vec{V} \tag{6}$$

The simulation was conducted using Computational Fluid Dynamics (CFD) software with the following configurations:

The turbulence model employed was the k-omega SST model. This model was chosen because the SST formulation effectively captures long, straight fluid flows, such as those found in flat regions, while the k-omega formulation enhances accuracy in regions with detailed flow structures and around suction areas. This selection ensures a balance between computational efficiency and predictive accuracy, particularly in capturing the complex interactions within the flow domain.

For the wall boundary condition, a no-slip condition was applied to model the reduction in fluid velocity near solid surfaces, generating a boundary layer effect. This condition was specifically assigned to the wall glass within the geometry to accurately represent the interaction between the fluid and solid surfaces.

At the inlet, a normal velocity condition was applied, where both velocity magnitude and liquid volume fraction (gas phase) were defined. To replicate realistic operating conditions, the inlet velocity was set to 1.8 m/s with an inlet temperature of 51°C.

For the outlet, a static pressure (outflow) condition was imposed at the outlet region to simulate the expected flow behaviour, ensuring numerical stability and consistency with experimental conditions.

Humidity modelling was activated to account for phase change effects, particularly the evaporation process, which is influenced by thermal conditions. The ambient temperature was set to 33°C to simulate the heat-induced vapour generation and assess the impact of humidity variations on evaporation rates.

Simulations focus on evaporation within a channel downstream of the air conditioner (AC) condenser, where airflow reaches temperatures up to 45°C. The airflow passes through the channel above the water surface, with varying cross-sectional areas of the channel set at 0.03, 0.024, 0.018, 0.012, and 0.006 m², as illustrated in Fig. 1.

Fig. 1 indicates the section to be simulated by red arrows, highlighting where water evaporates into vapour. Other areas are not included in the simulation as they are not the primary focus of this research. This study concentrates explicitly on water evaporation.

As mentioned earlier, simulation variations are achieved by altering the cross-sectional area of the channel without a Vortex Generator
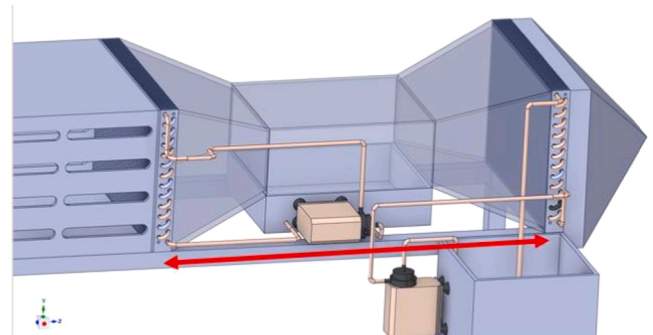

Fig. 1. Simulation model.

(NVG) and with a Vortex Generator (VG), as shown in Fig. 2.

The vortex generator used in this study is a V-shaped design, as it effectively directs airflow and generates efficient vortices without excessive flow resistance [20]. The choice of parameters is based on prior experimental and numerical studies. A height-to-channel height ratio of 0.47 was selected as it provides a balance between vortex strength and flow obstruction, ensuring enhanced mixing without inducing excessive drag [21], as pressure drop can be reduced by up to 43.9 % when the height ratio is less than 50 % [22]. The longitudinal pitch ratio of 0.18 was chosen because it maximizes vortex interaction, promoting turbulence intensity while preventing premature vortex dissipation [23]. The 30° angle of attack was selected as it has been shown to yield the best compromise between vortex strength, flow attachment, and overall thermal-hydraulic performance [24]. These design choices were validated through previous research and optimized for effective heat transfer and flow control.

The simulation model in this research simplifies the interface between air and water without fully capturing complex interfacial phenomena such as surface tension, evaporation-driven heat transfer at the molecular scale, and air-water interaction dynamics. Surface tension is excluded as its effect on large-scale evaporation is negligible, and grid independence testing shows that increasing the mesh from 160,000 to 900,000 elements improves evaporation by only 6.25 %, making its modelling inefficient. Similarly, evaporation-driven convective flows are omitted since the system is dominated by forced convection from AC condenser airflow, with a reduction in channel cross-sectional area increasing evaporation rates due to turbulence rather than natural convection. Humidity diffusion is also neglected as vapour transport is primarily driven by advection, with experiments showing that vortex generators enhance evaporation rates by 57 %, proving that turbulence has a greater impact than molecular diffusion. Despite its limitations, the model effectively demonstrates the impact of vortex generators on evaporation rates, aligning well with experimental data. These simplifications maintain computational efficiency, physical validity, and experimental consistency while accurately capturing the dominant evaporation mechanisms.

The modelling of the interaction between air and water during the evaporation process utilises a fluid domain, where warm air from the condenser flows over the water surface, influencing the evaporation rate, as illustrated in Fig. 3.

Fig. 3 illustrates the fluid domain (flow area) simulated in the CFD process. The analysed fluid domain is situated between the input (AC condenser) and the output, featuring two types of fluids: the air domain and the water domain. The initial water volume is 0.01 m³ .

In solving the fluid flow equations using CFD simulations, the fluid domain is divided into small elements (grid), referred to as mesh, as shown in Fig. 4.

Fig. 4 above illustrates the mesh utilised in the CFD simulation. The chosen element type is hexahedral, known for its structured grid that
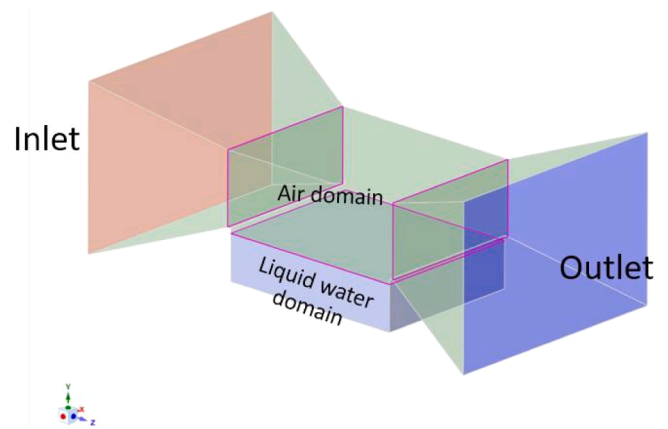

Fig. 3. Simulation domain.

enhances numerical stability and accuracy. This study considers the skewness and orthogonal quality values sufficient because they meet and exceed the standard thresholds used in CFD simulations. A skewness value below 0.25 is typically deemed acceptable, and an orthogonal quality value above 0.7 is considered good. The values of 0.08 and 0.98 ensure minimal numerical errors and optimal flow simulation, aligning with best practices in CFD modelling. A grid independence test was performed to ensure the reliability of the simulation results. This test determines whether the results are consistent across different mesh densities, confirming that the chosen mesh configuration does not significantly influence the findings.

Table 1 presents the outcomes of this grid independence test. A relative difference in results below 10 % establishes the validity of the simulation model used in this study. The 10 % threshold is commonly adopted in CFD studies as it represents a balance between computational cost and result accuracy, ensuring convergence of the numerical solution while maintaining efficiency [25]. This suggests that the numerical solution has achieved convergence. According to commonly applied CFD methodologies, a relative difference of less than 10 % is an acceptable criterion for grid independence [26]. Additionally, the residual analysis shows that the residual values consistently decrease and remain within an acceptable convergence threshold of 10^{-4} [27]. This ensures that the solution remains stable and is not significantly affected by further mesh refinement.

The selection of 600k mesh elements was based on the percentage difference analysis, which remained below 10 %, as well as the Richardson extrapolation method [28]. This technique is used to estimate numerical errors and ensure that further mesh refinement provides only marginal accuracy improvements compared to the significantly increased computational cost [29]. This methodology aligns with best practices in CFD grid validation, where excessive mesh refinement does
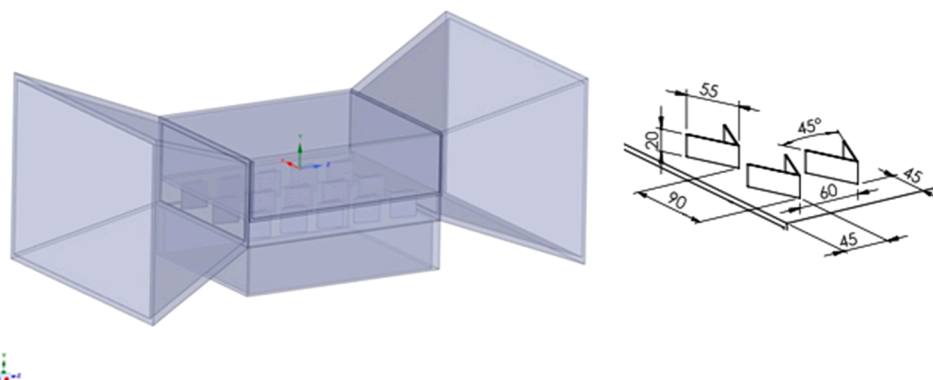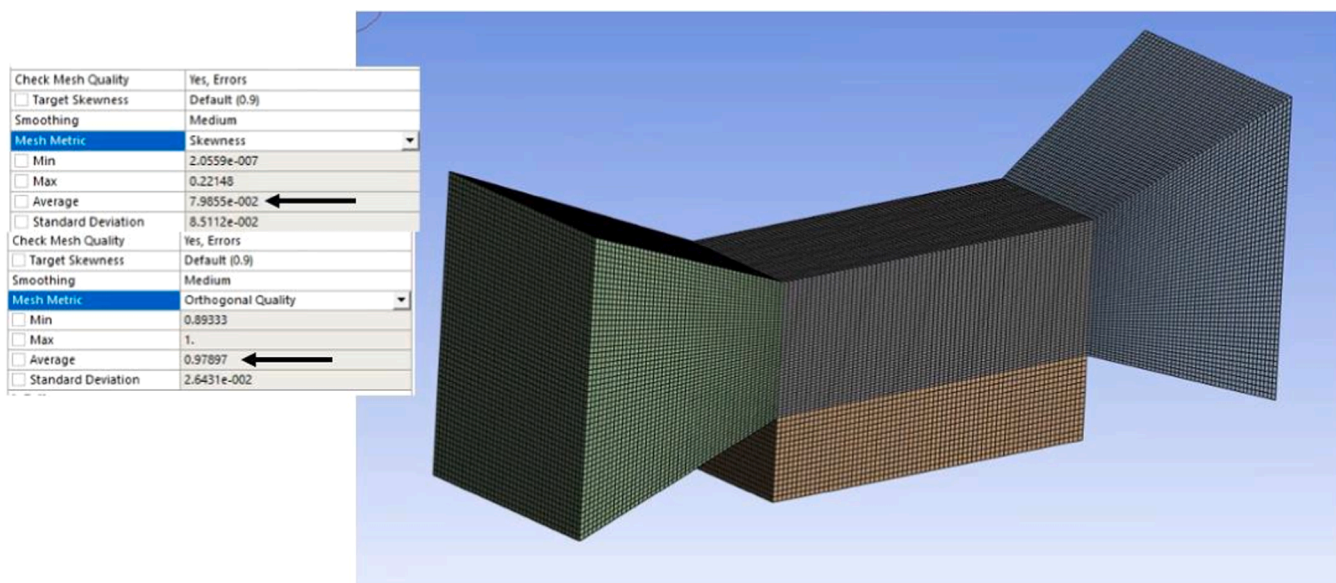

Fig. 2. Simulation variable.

Fig. 4. Simulation mesh.

Table 1
Grid independency test.

No	Mesh	Evaporation rate (kg/s.m^3)	%Difference
1	160k	1.12	-
2	250k	1.73	54.46
3	400k	2.27	31.21
4	600k	2.56	12.78
5	900k	2.72	6.25

Fig. 6. Experimental rig.

not substantially improve results but significantly increases computational load [30]. Therefore, the selection of 600k mesh elements is considered optimal, achieving a balance between computational efficiency and simulation accuracy. The generated mesh primarily consists of hexahedrons, offering high resolution and computational efficiency, as shown in Fig. 5. For detailed regions, polyhedral meshes are utilized due to their superior capability to conform to objects with high curvature.

The verification of CFD results can be conducted using data from experimental research or previous studies [31] to ensure that the CFD model accurately represents physical phenomena. In this study, the simulation results were verified using evaporation data obtained from experiments without a vortex generator, using an experimental rig shown in Fig. 6 and an experimental scheme in Fig. 7.

As shown in Fig. 7, feed water is pumped into the processed water tank using Pump 1 until it reaches capacity. If the tank reaches full capacity, excess water flows back to the feed tank through the return line.

When the water level decreases, the pump automatically refills the tank. Water from the processed water tank is then circulated using Pump 2 to the heat exchanger, where it is heated by the waste heat from the outdoor air conditioner (AC). The heated water returns to the processed
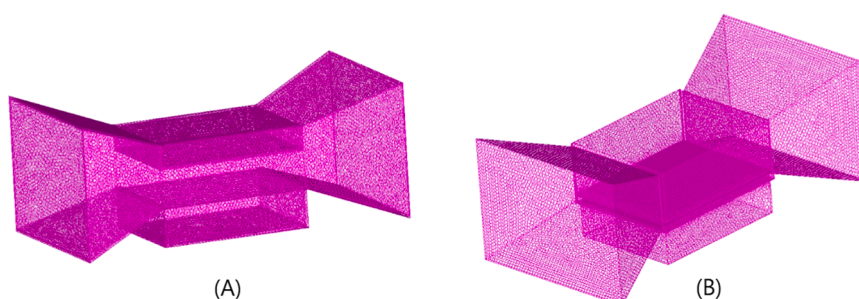

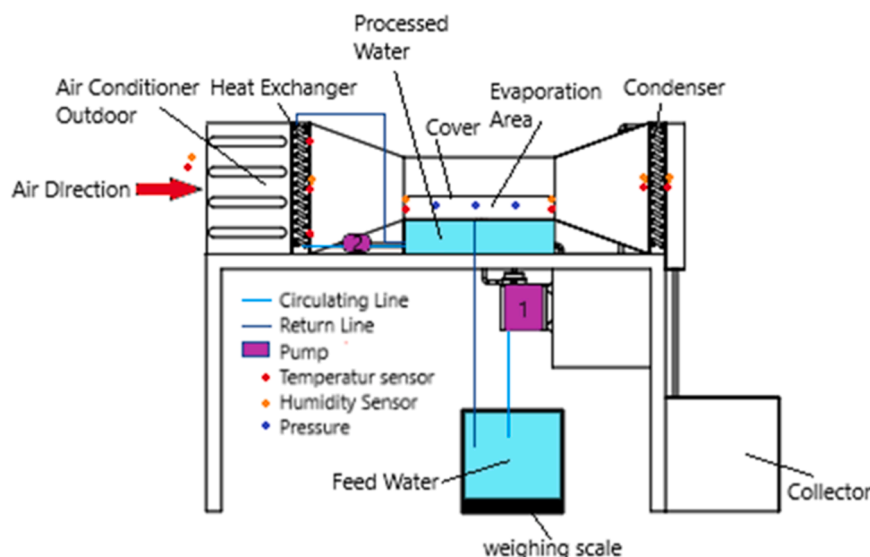**Fig. 5.** Simulation mesh without VG (A) and using VG (B).

Fig. 7. Experimental scheme.

tank, ensuring continuous thermal energy transfer. In addition to heating the water, the airflow from the outdoor AC is directed through the evaporation area to accelerate the evaporation process. The processed water undergoes phase change into vapour and moves along the airflow direction. The air, now carrying water vapour, is directed into the condenser, where the temperature is maintained at approximately 20°C. The condensed water is subsequently collected in a storage tank. The cover in the evaporation area is adjustable, allowing its height to be set between 2 cm and 14 cm above the water surface, which provides flexibility in optimizing the evaporation process. Multiple sensors are deployed to monitor system performance. Temperature is measured at various points, including the outlet of the outdoor AC, the inlet and outlet of the evaporation area, the inlet and outlet of the condenser, and the ambient environment, using PT100 sensors (-50°C to 110°C, ± 0.1°C accuracy). Humidity levels are recorded at corresponding points using a digital hygrometer (10 %–99 % range, 1 % resolution, ± 1 % accuracy). A weighing scale with a capacity of 20 kg (0–20 kg range, 0.5 g resolution) is used to measure the weight of water in the feed tank. The measurement begins once the processed water tank is fully filled. The reduction in water weight is used to quantify the evaporation occurring in the evaporation area. Air velocity is monitored using an anemometer GM-816 (0–30 m/s range, 0.1 m/s resolution). Additionally, the pressure in the evaporation area is measured using a Pressure Meter PCE-PDA 1 L to ensure optimal operating conditions.

3. Results

The simulation results presented in this article focus on the airflow velocity as influenced by the reduction in cross-sectional area and the corresponding evaporation rates. This analysis encompasses scenarios both without vortex generators (NVG) and with vortex generators (VG).

The investigation highlights how variations in the channel's cross-sectional area impact the airflow's velocity. As the area decreases, the airflow velocity tends to increase due to fluid dynamics principles, particularly the continuity equation, which states that the mass flow rate must remain constant from one flow cross-section to another.

The comparative results between the two configurations—one using vortex generators and the other without—will provide insights into the effectiveness of vortex generators in enhancing the evaporation process. This study aims to contribute to the understanding of optimising desalination techniques, particularly for applications in coastal areas where water scarcity is a critical issue. By demonstrating the impact of airflow velocity on evaporation rates, the findings will highlight the importance

of flow dynamics in improving desalination efficiency.

The increase in airflow velocity caused by the vortex generator, as shown in Table 2, is closely related to the evaporation process. Table 2 illustrates that airflow velocity increases as the cross-sectional area of the channel decreases. When vortex generators are applied to the channel, the airflow velocity increases significantly compared to the channel without vortex generators (NVG). This occurs because vortex generators create longitudinal vortices that disturb the boundary layer, reduce thickness, and enhance fluid mixing. As a result, higher airflow velocity leads to more efficient removal of water vapour from the surface, accelerating the evaporation process. Additionally, the increased airflow velocity, as reflected in the data from Table 2, also accelerates the transfer of thermal energy from the water surface to the surrounding air.

With better flow distribution and higher turbulence, the heat absorbed from the water surface can be transferred more efficiently to the air, ultimately speeding up evaporation. Longitudinal vortices can significantly improve flow distribution and momentum transfer in small channels, enhancing evaporation efficiency by optimising pressure distribution within the microchannel [32]. Moreover, these findings align with other research, showing that decreasing the cross-sectional area of the channel improves flow distribution and momentum transfer in microchannel systems, further enhancing evaporation efficiency [33]. Thus, the implementation of vortex generators not only optimises thermal and fluid performance in systems such as heat exchangers and cooling mechanisms and enhances evaporation rates, as demonstrated in Table 3.

Table 3 compares the evaporation rates for the NVG and VG configurations. Channels equipped with vortex generators show significantly higher evaporation rates. The average increase in the evaporation rate, approximately 57 %, is due to enhanced fluid mixing and continuous disruption of the thermal boundary layer, which improves heat transfer efficiency.

There are two key implications of this increase in evaporation rate. First, improved mass transfer facilitates the removal of saturated air near the water surface, allowing for higher evaporation efficiency. Second, disrupting the stagnant air layer near the liquid surface ensures a continuous supply of dry air, creating a higher concentration gradient for evaporation. These findings emphasise the importance of vortex generators in applications such as desalination, where optimising evaporation efficiency is crucial. Micro-vortices can accelerate evaporation by increasing turbulence and reducing boundary layer thickness [34]. The higher evaporation rates observed in vortex-induced systems

Table 2
Velocity contour.

cross-sectional area	NVG	VG
0.03 m²		
0.024 m²		
0.018 m²		
0.012 m²		
0.006 m²		
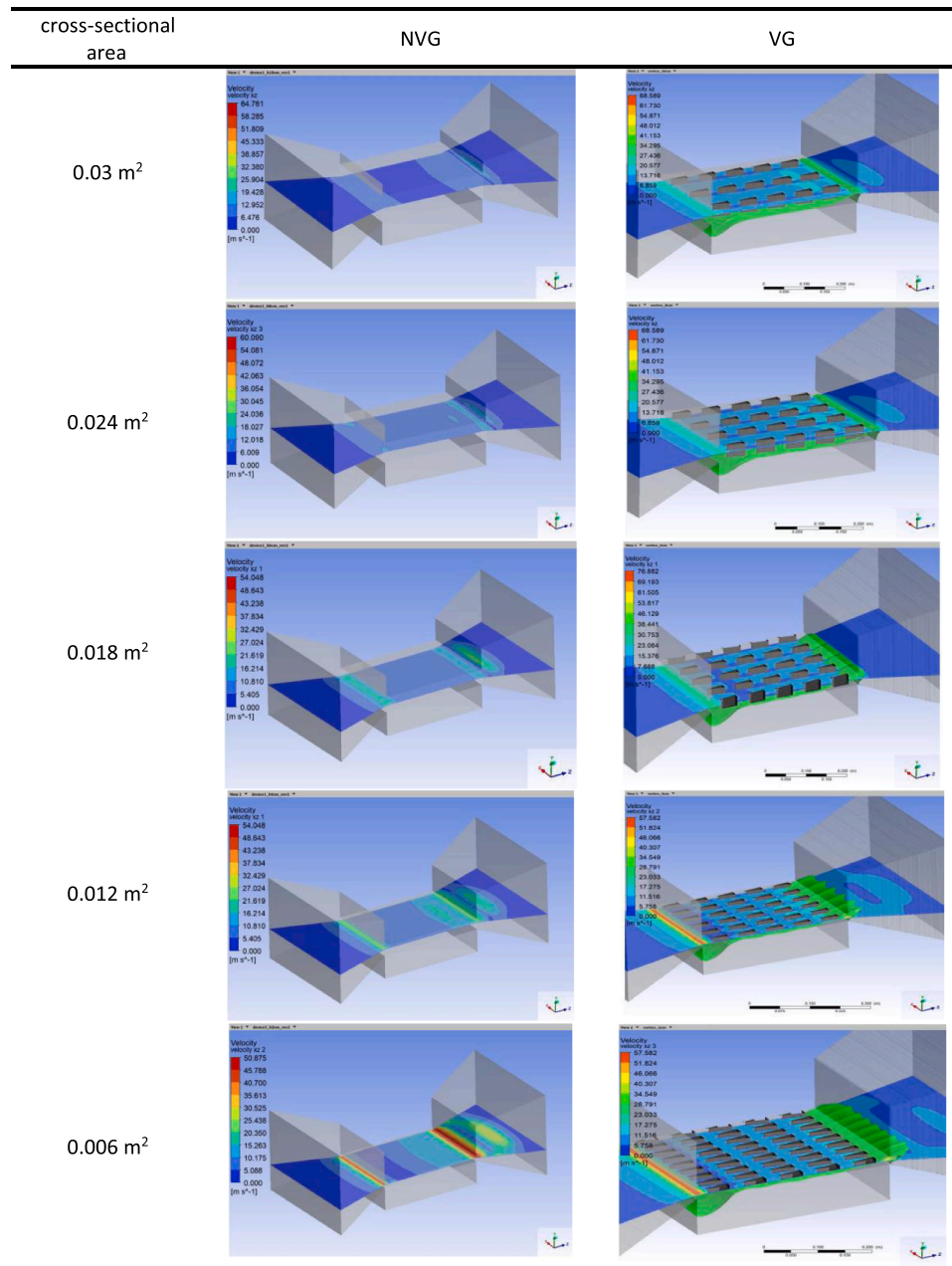
are closely related to the reduction of the thermal boundary layer thickness, which speeds up the transport of water molecules from the liquid surface to the airflow [35].

This enhanced airflow leads to a more efficient evaporation process, as the constant replacement of saturated air with drier air increases the evaporation rate. The findings presented in Table 3 highlight the positive impact of vortex generators on evaporation efficiency, making them a valuable component in systems designed for desalination or other thermal applications. Additionally, the increased evaporation rates observed in the presence of vortex generators contribute to the effectiveness of water desalination techniques and offer potential improvements in various industrial processes where evaporation is a key mechanism.

To validate the CFD results, the evaporation rate obtained from the simulation was compared with experimental data. This comparison is presented in Table 4, which displays the deviation between CFD results and experimental data.

This comparison shows that the maximum deviation between the CFD results and the experiment is 6.99 %, which is still within the acceptable error range for CFD studies, typically 5–10 % [35]. These findings confirm that the numerical model used is capable of reliably representing the physical phenomena, thereby increasing confidence in the simulation results [36],[37].

Furthermore, the evaporation results from the simulation were verified against the experimental evaporation data, as presented in Fig. 8.

Fig. 8 shows that the evaporation rates from the simulation closely match the experimental results, forming an almost linear relationship with a coefficient of determination (R²) of 0.9804. This indicates that the simulation results align well with the experimental data [38], with a
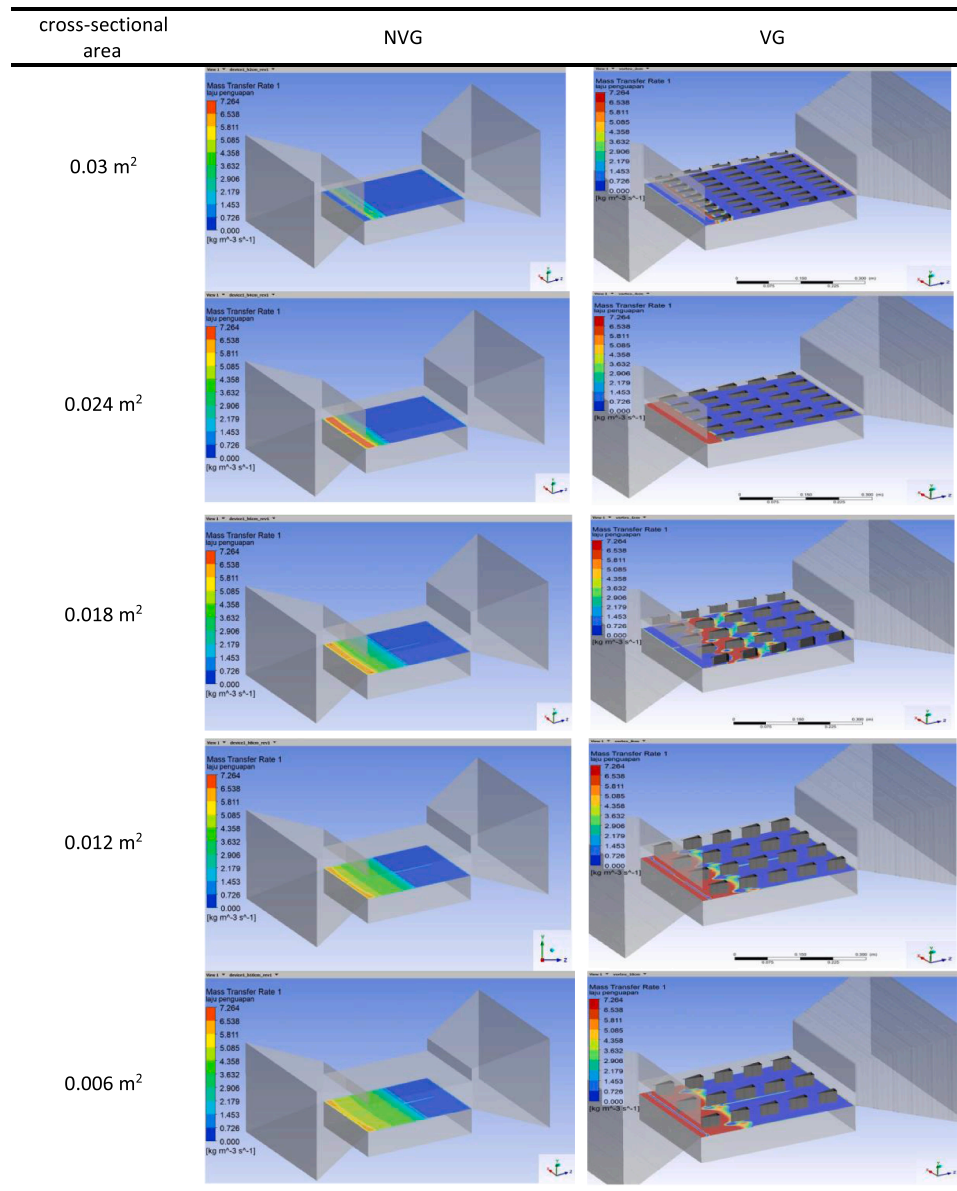
Table 3
Evaporation rate.

cross-sectional area	NVG	VG
0.03 m²		
0.024 m²		
0.018 m²		
0.012 m²		
0.006 m²		

Table 4
Result deviation.

Configuration	Evaporation Rate (CFD) (kg/s·m³)	Evaporation Rate (Experiment) (kg/s·m³)	Deviation (%)
NVG	2.56	2.42	5.79
VG	3.98	3.72	6.99

Fig. 8. Simulation-based model verification against experimental data.

deviation of only 7.1 %. The high agreement between the simulation and experimental data demonstrates that the CFD simulation approach is reliable for predicting VG's mass transfer enhancement effects. Low deviation in CFD simulations when modelling the effects of vortices on mass and heat transfer [39]. Subsequently, the simulation results for evaporation without a Vortex Generator (NVG) are compared to those with a Vortex Generator (VG), as shown in Fig. 9.

The findings presented in Fig. 9 further validate the analysis, demonstrating the impact of vortex generators on evaporation rates. The
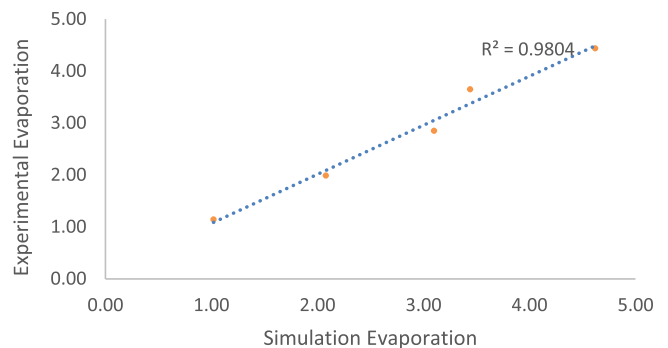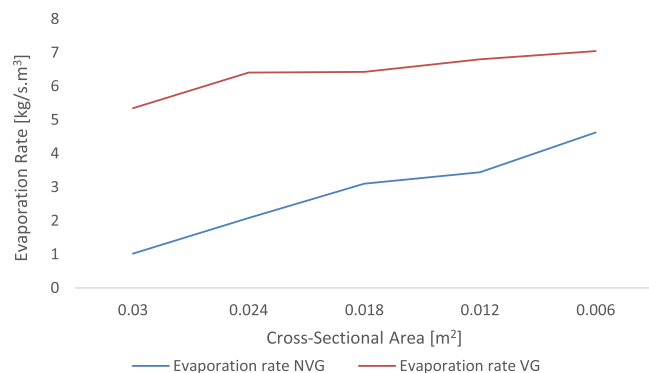
O. Heriyani et al.

Fig. 9. Evaporation rate NVG and VG.

simulation results depicted in Fig. 9 reveal that using vortex generators increases the evaporation rate by an average of 57 % compared to systems without vortex generators. This enhancement is primarily due to the effect of vortex generators in increasing the flow velocity along the surface, which causes flow instability (turbulence) and the development of boundary layers and vortices [40]. These effects, in turn, amplify the temperature gradient between the surface and the surrounding air [41].

The research findings indicate that applying vortex generators (VG) in evaporation systems, such as those used in desalination or industrial drying processes, provides significant advantages in terms of thermal efficiency. VG increases the evaporation rate, reducing operational time and energy consumption. The optimisation of VG design holds great potential for further improving thermal efficiency. The optimal VG geometry can maximise evaporation rates and heat transfer under various environmental conditions [42]. VG significantly enhances evaporation efficiency in desalination processes [43], thereby lowering operational costs.

Evaporation occurring within the channel can be described by the equation $J = K_m (P_s - P_a)$, where J represents the mass transfer rate due to evaporation and k_m is the mass transfer coefficient. P_s and P_a are saturation vapour pressure at the surface and partial vapour pressure of the surrounding air, respectively. The vortex generators enhance the mass transfer rate by promoting turbulence and improving the mixing of the fluid, which in turn increases the effective mass transfer coefficient k_m. This leads to a more efficient transfer of vapour from the surface to the surrounding air, driven by the vapour pressure difference. The influence of the vortex generators results in higher evaporation rates compared to a system without such enhancements.

Implementing VG in evaporation-dependent systems, such as evaporative cooling or industrial drying, provides substantial benefits. VG accelerates the evaporation process and reduces the additional energy required to maintain the temperature gradient, thus improving operational efficiency. This increase in evaporation rates also enables the design of surfaces involved in heat and mass transfer to become more compact without compromising performance. As a result, material costs can be reduced, and overall system performance can be enhanced. Therefore, the impact of vortex generators on flow and evaporation offers an efficient and innovative approach to improving the performance of thermal and fluid systems.

4. Conclusions

This study confirms that vortex generators significantly improve evaporation rates in desalination systems by harnessing waste heat from air conditioners. The results indicate an average increase of 57 % in evaporation rates when vortex generators are employed, attributed to the induced turbulence that improves fluid mixing and thermal energy transfer. This research highlights the effectiveness of vortex generators in optimising airflow dynamics, leading to more efficient heat transfer and evaporation processes.

From a scientific perspective, this work contributes to understanding fluid dynamics and heat transfer mechanisms in evaporative systems. It provides a novel approach for utilising existing household technologies, such as air conditioning units, to address pressing issues related to freshwater scarcity, particularly in coastal regions. Additionally, the findings pave the way for further exploration of innovative solutions in thermal management, potentially influencing the design and efficiency of future systems in domestic and industrial applications. The study encourages the adoption of vortex generators as a feasible method for improving thermal efficiency, thereby promoting sustainable practices in water desalination and environmental management.

CRediT authorship contribution statement

Oktarina Heriyani: Writing – original draft. **Dan Mugisidi:** Supervision, Methodology, Conceptualization. **Rifky:** Writing – review & editing.

Declaration of Competing Interest

The authors declare that they have no known competing financial interests or personal relationships that could have appeared to influence the work reported in this paper.

Acknowledgement

Data availability

Data will be made available on request.

References

[1] Schewe J, Heinke J, Gerten D, Haddeland I, Arnell NW. Multimodel assessment of water scarcity under climate change. *Proc Natl Acad Sci USA* 2014;111(9):3245–50. https://doi.org/10.1073/pnas.1222460110.

[2] Belessiotis V, Kalogirou S, Delyannis Emmy. Thermal Solar Desalination - Methods and Systems. London: Academic Press; 2016.

[3] Pauli BJ. The Flint water crisis. Wiley Interdiscip Rev: Water May 2020;7(3). https://doi.org/10.1002/WAT2.1420.

[4] LIPI, "Indonesia Negeri Tropis, Tapi Krisis Air Bersih di Kawasan Pesisir Terjadi?" Accessed: Aug. 05, 2022. [Online]. Available: ⟨http://lipi.go.id/lipimedia/Indonesia-Negeri-Tropis-Tapi-Krisis-Air-Bersih-di-Kawasan-Pesisir-Terjadi/20218⟩.

[5] V. Masson-Delmotte et al., "Global warming of 1.5°C; An IPCC Special Report on the impacts of global warming of 1.5°C," 2019. [Online]. Available: ⟨www.environmentalgraphiti.org⟩.

[6] Pielkejr BRA, Landsea C, Mayfield M, Layer J, Pasch R. Hurricanes and Global Warming. American Meteorological Society; 2005. https://doi.org/10.1175/BAMS-86-II-1571.

[7] Y. Hwang, R. Radermacher, and W. Kopko, "An experimental evaluation of a residential-sized evaporatively cooled condenser," 2001. [Online]. Available: ⟨www.elsevier.com/locate/ijrefrig⟩.

[8] Wirangga Ristanto, Mugisidi Dan, Sayuti Adi Tegar, Heriyani Oktarina. The impact of wind speed on the rate of water evaporation in a desalination chamber. J Adv Res Fluid Mech Therm Sci Jun. 2023;106(1):39–50. https://doi.org/10.37934/arfmts.106.1.3950.

[9] Byrne P, Ait Oumeziane Y, Serres L, Mare T. Study of a heat pump for simultaneous cooling and desalination. Appl Mech Mater Jan. 2016;819:152–9. https://doi.org/10.4028/www.scientific.net/amm.819.152.

[10] Srinivas T, Saxena A, Baba SV, Kukreja R. Experimental and simulation studies on heat pump integration two stage desalination and cooling system. Energy Nexus Sep. 2023;11. https://doi.org/10.1016/j.nexus.2023.100221.

[11] Yang J, Zhang C, Lin X, Zhang Z, Yang L. Wastewater desalination system utilizing a low-temperature heat pump. Int J Energy Res Mar. 2018;42(3):1132–8. https://doi.org/10.1002/er.3909.

[12] Dehghani S, Date A, Akbarzadeh A. Performance analysis of a heat pump driven humidification-dehumidification desalination system. Desalination Nov. 2018;445:95–104. https://doi.org/10.1016/j.desal.2018.07.033.

[13] Shafii MB, Jafargholi H, Faegh M. Experimental investigation of heat recovery in a humidification-dehumidification desalination system via a heat pump. Desalination Jul. 2018;437:81–8. https://doi.org/10.1016/j.desal.2018.03.004.

[14] Amarloo A, Shafii MB. Enhanced solar still condensation by using a radiative cooling system and phase change material. Desalination 2019;467(June):43–50. https://doi.org/10.1016/j.desal.2019.05.017.

[15] Md Salleh MF, Gholami A, Wahid MA. Numerical evaluation of thermal hydraulic performance in fin-and-tube heat exchangers with various vortex generator geometries arranged in common-flow-up. J Heat Transf 2019;141(2). https://doi.org/10.1115/1.4041832.

[16] O. Heriyani, D. Mugisidi, and I. Hilmi, Effect of cylinder surface roughness, *SINTEK*, vol. 14, no. 2, pp. 94–98, 2020, doi: 10.24853/sintek.14.2.94-98.

[17] Sumatri F, Fitri M. Perancangan alat uji vortex bebas dan vortex paksa. Zona Mesin 2017;8(2):1–9.

[18] Mugisidi D, Heriyani O, Gunawan PH, Apriani D. Performance improvement of a forced draught cooling tower using a vortex generator. CFD Lett 2021;13(1):45–57. https://doi.org/10.37934/cfdl.13.1.4557.

[19] Mugisidi D, et al. Iron sand as a heat absorber to enhance performance of a single-basin solar still. J Adv Res Fluid Mech Therm Sci 2020;70(1):125–35. https://doi.org/10.37934/arfmts.70.1.125135.

[20] H. Tebbiche, H. Tebbiche, and M. Boutoudj, "Aerodynamic drag reduction by turbulent flow control with vortex generators," in 5th International Symposium on Aircraft Materials, Marrakech, Aug. 2014. [Online]. Available: ⟨https://www.researchgate.net/publication/292967041⟩.

[21] Han Z, Xu Z, Qu H. Parametric study of the particulate fouling characteristics of vortex generators in a heat exchanger. Appl Therm Eng 2020. https://doi.org/10.1016/j.applthermaleng.2019.114735.

[22] Chen L, Zhang XR, Okajima J, Komiya A, Maruyama S. Numerical simulation of stability behaviors and heat transfer characteristics for near-critical fluid microchannel flows. Energy Convers Manag Feb. 2016;110:407–18. https://doi.org/10.1016/J.ENCONMAN.2015.12.031.

[23] Dietz CF, Henze M, Neumann SO, Von Wolfersdorf J, Weigand B. The effects of vortex structures on heat transfer and flow field behind arrays of vortex generators. J Enhanc Heat Transf 2009. https://doi.org/10.1615/JEnhHeatTransf.v16.i2.60.

[24] Min C, Qi C, Wang E, Tian L, Qin Y. Numerical investigation of turbulent flow and heat transfer in a channel with novel longitudinal vortex generators. Int J Heat Mass Transf 2012;55(23–24):7268–77. https://doi.org/10.1016/j.ijheatmasstransfer.2012.07.055.

[25] Md Salleh MF, Gholami A, Wahid MA. Numerical evaluation of thermal hydraulic performance in fin-and-tube heat exchangers with various vortex generator geometries arranged in common-flow-down or common-flow-up. J Heat Transf Feb. 2019;141(2). https://doi.org/10.1115/1.4041832/477191.

[26] Fu H, Sun H, Yang L, Yan L, Luan Y, Magagnato F. Effects of the configuration of the delta winglet longitudinal vortex generators and channel height on flow and heat transfer in minichannels. Appl Therm Eng Jun. 2023;227:120401. https://doi.org/10.1016/J.APPLTHERMALENG.2023.120401.

[27] Yang J, et al. Numerical study of evaporation–condensation heat transfer in finned double pipe heat exchangers. Case Stud Therm Eng Jan. 2025;65:105667. https://doi.org/10.1016/J.CSITE.2024.105667.

[28] Min C, Qi C, Wang E, Tian L, Qin Y. Numerical investigation of turbulent flow and heat transfer in a channel with novel longitudinal vortex generators. Int J Heat Mass Transf Nov. 2012;55(23–24):7268–77. https://doi.org/10.1016/J.IJHEATMASSTRANSFER.2012.07.055.

[29] Manda U, Mazumdar S, Peles Y. Effects of cross-sectional shape on flow and heat transfer of the laminar flow of supercritical carbon dioxide inside horizontal microchannels. Int J Therm Sci Jul. 2024;201:108992. https://doi.org/10.1016/J.IJTHERMALSCI.2024.108992.

[30] Oh Y, Kim K. Effects of position and geometry of curved vortex generators on fin-tube heat-exchanger performance characteristics. Appl Therm Eng May 2021;189:116736. https://doi.org/10.1016/J.APPLTHERMALENG.2021.116736.

[31] Heriyani O, Djaeni M, Syaiful. Thermal-hydraulic performance analysis by means of rectangular winglet vortex generators in a channel: an experimental study. Eur J Eng Technol Res 2021;6(3):150–3. https://doi.org/10.24018/ejers.2021.6.3.2424.

[32] Fu H, Sun H, Yang L, Yan L, Luan Y, Magagnato F. Effects of the configuration of the delta winglet longitudinal vortex generators and channel height on flow and heat transfer in minichannels. Appl Therm Eng Jun. 2023;227:120401. https://doi.org/10.1016/J.APPLTHERMALENG.2023.120401.

[33] Hekmatara M, Kharati-Koopaee M. Numerical study of the influence of pin fin arrangement and volume fraction on the heat transfer and fluid flow phenomena within open microchannels. Int Commun Heat Mass Transf Jun. 2024;155:107595. https://doi.org/10.1016/J.ICHEATMASSTRANSFER.2024.107595.

[34] Misyura SY, Kuznetsov GV, Volkov RS, Morozov VS. Droplet evaporation on a structured surface: the role of near wall vortexes in heat and mass transfer. Int J Heat Mass Transf Feb. 2020;148:119126. https://doi.org/10.1016/J.IJHEATMASSTRANSFER.2019.119126.

[35] Sommers AD, Jacobi AM. Air-side heat transfer enhancement of a refrigerator evaporator using vortex generation. Int J Refrig Nov. 2005;28(7):1006–17. https://doi.org/10.1016/J.IJREFRIG.2005.04.003.

[36] Feng Z, et al. Experimental and numerical investigations on the effects of insertion-type longitudinal vortex generators on flow and heat transfer characteristics in square minichannels. Energy Sep. 2023;278:127855. https://doi.org/10.1016/J.ENERGY.2023.127855.

[37] Saad MA, Tourab AE, Salem MH, Ismail A. Multifaceted analytical and computational fluid dynamics investigations of vortex tube technology for the optimization of seawater desalination efficiency. Results Eng Mar. 2025;25:104004. https://doi.org/10.1016/J.RINENG.2025.104004.

[38] Di Bucchianico Alessandro. Coefficient of Determination (R2). Encyclopedia of Statistics in Quality and Reliability. Wiley Online Library; 2008. https://doi.org/10.1002/9780470061572.eqr173.

[39] Guo Y, et al. Vortex augmented heat and humidity energy extraction and the variation of vortex strength behind the string grid. Fuel May 2025;387:134297. https://doi.org/10.1016/J.FUEL.2025.134297.

[40] Fiebig M. Vortices, generators and heat transfer. Chem Eng Res Des 1998;76(2):108–23. https://doi.org/10.1205/026387698524686.

[41] Lemenand T, Habchi C, Della Valle D, Peerhossaini H. Vorticity and convective heat transfer downstream of a vortex generator. Int J Therm Sci Mar. 2018;125:342–9. https://doi.org/10.1016/j.ijthermalsci.2017.11.021.

[42] Batista J, Trp A, Lenic K, Kirincic M. The influence of geometry parameters of rectangular vortex generators on the air-to-water fin-and-tube heat exchanger efficiency enhancement. Int Commun Heat Mass Transf Mar. 2025;162:108647. https://doi.org/10.1016/J.ICHEATMASSTRANSFER.2025.108647.

[43] Mugisidi D, Heriyani O. Improving the performance of a forced-flow desalination unit using a vortex generator. CFD Lett Oct. 2024;16(10):81–93. https://doi.org/10.37934/cfdl.16.10.8193.